Simple Chemical Bath Deposited Zinc Oxide Nanoflowers and their Applications for Extended-Gate FET pH Sensor

A. B. Rosli [1,2], A. S. Ismail[1], Z. Awang [3], M. F. Abdul Khalid [3], S. S. Shariffudin[1] and S. H. Herman [2,3*]

***Abstract*—Zinc Oxide (ZnO) nanostructures deposited using simple chemical bath deposition (CBD) at different deposition time ranging from 1 to 4 hours on indium tin oxide (ITO) substrates are proposed as sensing membrane of extended-gate field effect transistor (EGFET) pH sensor. The ZnO nanostructures were grown without any seed or catalyst layer. The deposited samples were characterized on their physical properties in order to investigate the correlation between physical properties and pH sensing behavior based on the influence of various deposition time to the physical properties. It is evident from the FESEM result that the nanostructures growth density is directly proportional to the growth time. Same goes on crystallinity quality of the samples that shows the same pattern as growth density. The physical properties of the ZnO nanostructures can be related to the immersion time and in turn influence the pH sensor performance. All deposited samples showed the ability to be applied as the sensing material for the EGFET pH sensor with the highest performance was obtained from the 3-hours sample having sensitivity of 56.0 mV/pH and 0.9997 linearity. The high sensitivity obtained from the 3-hour sample is related to high growth density of ZnO nanostructures that provide high surface area which facilities more contact between sensing membrane and pH buffer for ion adsorptions.**

***Index Terms*—ZnO Nanostructures, Chemical Bath Deposition (CBD), Deposition Time, EGFET**

I. INTRODUCTION

pH detection becomes a fundamental measurement in many fields including industries, medical, and environmental. The pH level can be determined by measuring the concentration of hydrogen ions (H^+). Since many chemical and biological reaction are dependent on concentration of H^+ ion, therefore it becomes a priority to researchers to produce pH sensors with sensitive and reliable characteristics. Extended gate field effect transistor (EGFET) pH sensor has attracted many researchers since it offers several advantages that fulfill the requirement of pH sensors [1, 2]. The EGFET consists of metal oxide semiconductor field effect transistor (MOSFET) isolated from electrolyte solution and the sensing membrane that is immersed together with the reference electrode (RE) in the electrolyte solutions [3]. Most of the study reported on EGFET pH sensors was focusing on the sensing membrane material [4-6].

Metal oxide semiconductor materials become one of the common material used for sensing membrane due to their excellent properties which are chemically stable and ease to fabricate [7]. The size and morphology of metal oxide semiconductor material also can be controlled for surface modification [8-11]. Fayroz A.Sabah et al has deposited Copper(II) sulfide CuS as EGFET sensing membrane at different post annealing time. They found that the sensitivity of CuS is influenced by the CuS growth morphology. The optimum sensitivity was found at 30 min annealed sample with 27.8 mV/pH of sensitivity value [1]. Besides that M. A. Zulkefle et al has studied the porous TiO_2 as EGFET sensing membrane [12]. The results obtained shows the porous TiO_2 has ability as pH sensor sensing membrane with sensitivity and linearity of 19.30 mV/pH and 0.9950 respectively. From previous reserchers, it can be concluded that the growth morphology of metal oxide play a significant role in enhance the EGFET sensing performance [13-15]. Having an outstanding characteristics in terms of electrical and sensing properties, the zinc oxide (ZnO) becomes one of the promising metal oxide semiconductor material as the sensing membrane [16]. Besides that, ZnO also has variety of nanostructure morphologies that provides large surface area which contributes to favourable sensing performance. Until now, extensive researches have been done to produce the sensing material with novel structures that can improve the sensing performance [17]. This surface structures are depending on the synthesis methods and their conditions [16]. Among the synthesis methods that have been reported, solution-based methods have emerged as an excellent method in producing high quality ZnO nanostructures at lower deposition temperature that are required for device applications. The deposition time during deposition process was reported to play significant roles that would influenced the growth morphologies of ZnO nanostructures and contributes to better devices performance [18-21]. However, there are still limited report on this effect on EGFET pH sensor performance.

Therefore, in this paper, the influence of the deposition time of ZnO nanostructures sensing membrane on the EGFET pH

This manuscript is submitted on 8th November 2018 and accepted on 28th February 2019.

1 NANO-ElecTronic Centre, Faculty of Electrical Engineering, Universiti Teknologi MARA, 40450, Shah Alam, Selangor, Malaysia

2 Integrated Sensors Research Group, Faculty of Electrical Engineering, Universiti Teknologi MARA, 40450 Shah Alam, Selangor, Malaysia

3 Microwave Research Institute, Universiti Teknologi MARA, 40450 Shah Alam, Selangor, Malaysia

* *Correspondence: hana1617@salam.uitm.edu.my; Tel.: +603-55436041*

sensor performance is reported. The ZnO nanostructures was growth using chemical bath deposition (CBD) method at different deposition time ranging from 1 to 4 hours and further applied as the sensing membrane for EGFET pH sensor.

II. Material and Methods

A. ZnO Nanostructure Deposition

In this work, the CBD method was used to fabricate ZnO nanostructures. 0.23 g zinc nitrate hexahydrate [Zn $(N0_3)_2$. $_6H_2O$] and 0.11 g of hexamethylenetetramine (HMT, $(C_6H_{12}N_4)$) were dissolved in 100 ml of deionized (DI) water. Prior to the stirring process, the solution was sonicated for 30 mins in ultrasonic bath. In order to ensure the solution was dispersed, the mixture was stirred using magnetic stirrer at 300 rpm at room temperature for 3 hours.1 cm × 2 cm indium tin oxide (ITO) coated glass was used as the substrate due to the high conductivity of ITO which is needed to complete the circuitry of the EGFET pH sensor setup. The ITO substrate was immersed in ZnO solution and placed in water bath at 95 ºC with the deposition time varied from 1 to 4 hours. After the deposition process, the deposited samples was cooled at room temperature for 14 hours followed by drying and annealing treatment for 30 mins at 500 ºC. The ZnO nanostructures was deposited to form 1 cm × 1 cm sensing area while the rest of the ITO substrate surface was left uncoated.

B. Sample Characterization

Field- emission scanning electron microscope (FESEM, JSM-7600F) and X-ray diffraction (PANalytical X'Pert PRO XRD) with monochromatic Cu Ka radiation (λ = 0.154 nm) were used to investigate the surface morphology and crystalline properties of the ZnO nanostructures respectively. For pH sensing capability, the uncoated conductive area of the ITO substrate surface was connected to a metal wire using silver paste and encapsulation was done to further strengthen the contact and avoid leakage of the solution during measurement process. The other end of the wire was connected to the gate of a commercialized n type FET. The sensing membrane and a reference electrode (Ag/AgCl) were dipped together into different ready-made J.T. Beaker pH buffer solutions of pH 4, 7 and 10. Fig.1 Shows the measurement setup of EGFET pH sensor. The Semiconductor Device Analyzer model Keysight B1500A was used to measure current-voltage (I_D-V_{REF}) characteristics of the deposited samples. The source (S) and drain (D) terminal were connected to source measure unit (SMU) 1 and 2 while the reference electrode was connected to SMU 3 as shown in Fig. 1. From the transfer curve analysis, the gate voltage versus pH graph was plotted based on gate voltage at 100 µA for each pH level. The sensor sensitivity was obtained from the V_{REF} -pH graph slope and the linearity was the linear regression (R^2).

III. Results & Discussion

A. ZnO Nanostructures Characteristics

The FESEM images of the synthesized ZnO nanostructures are shown in Fig.2. It is clear that for the sample deposited at 1 and 2 hours, the nanostructures are small and distributed across the substrate surface as shown in Fig.2 (a) and (b) respectively. Most of the nanostructures are in the form of rods. There is no distinct difference that can be observed between the samples prepared at 1 and 2 hours, but increasing the deposition time to 3 hours caused the agglomeration of ZnO nanorods and formed ZnO nanoflowers. The growth density of ZnO nanoflower on the sample deposited at 3 hours is highest compared to other samples, however, the nanostructure growth density reduces for the sample deposited at 4 hours (Fig. 2 (d)). This can be schematically explained in Fig. 3.

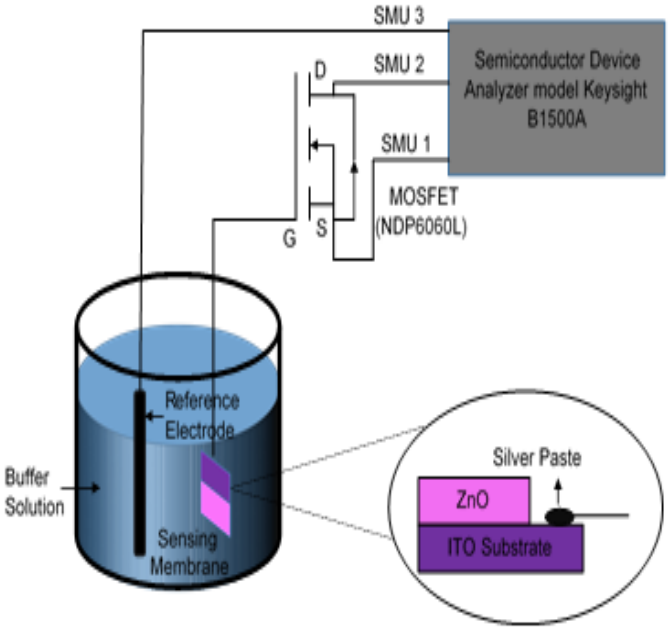

Fig. 1.EGFET sensor measurement setup

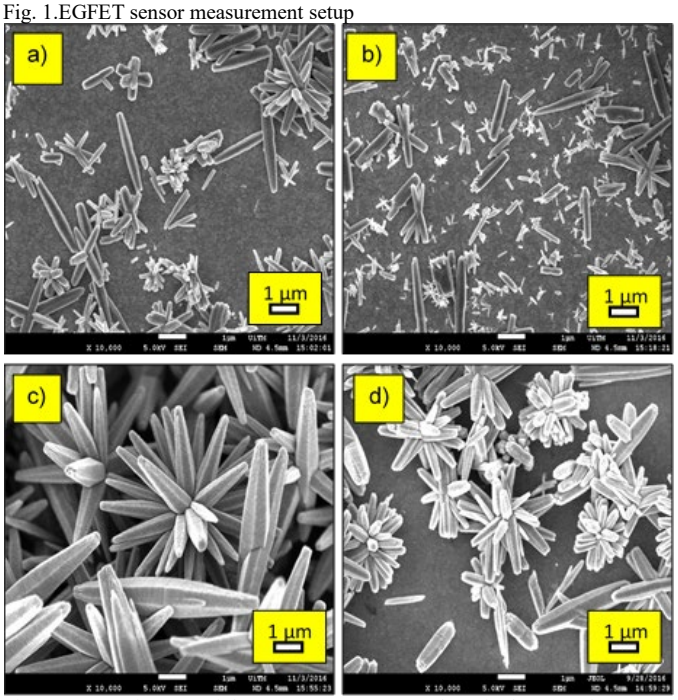

Fig. 2.FESEM images of the ZnO nanostructures deposited at a) 1, b) 2 , c) 3 and d) 4 hours

IV. Results & Discussion

TABLE I
THE MORPHOLOGICAL PARAMETERS FOR EACH THIN FILM AT DIFFERENT DEPOSITION TIME

Deposition Time (Hour)	Diameter (nm)	Length (nm)
1	75-125	175-450
2	100-150	550-1075
3	225-425	875-1475
4	150-400	700-1200

A. ZnO Nanostructures Characteristics

The FESEM images of the synthesized ZnO nanostructures are shown in Fig.2. It is clear that for the sample deposited at 1 and 2 hours, the nanostructures are small and distributed across the substrate surface as shown in Fig.2 (a) and (b) respectively. Most of the nanostructures are in the form of rods. There is no distinct difference that can be observed between the samples prepared at 1 and 2 hours, but increasing the deposition time to 3 hours caused the agglomeration of ZnO nanorods and formed ZnO nanoflowers. The growth density of ZnO nanoflower on the sample deposited at 3 hours is highest compared to other samples, however, the nanostructure growth density reduces for the sample deposited at 4 hours (Fig. 2 (d)). This can be schematically explained in Fig. 3.

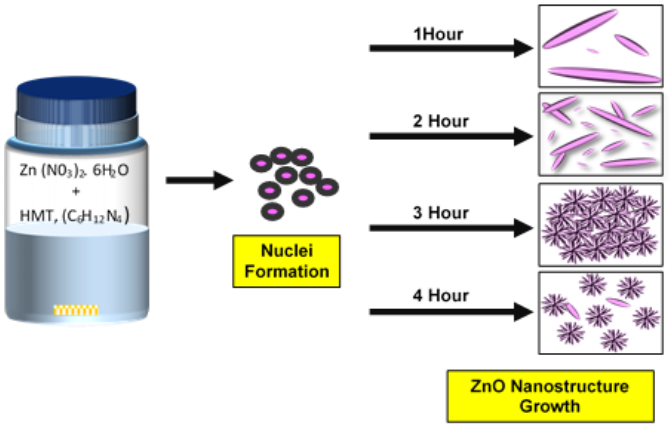

Fig. 3.FESEM images of the ZnO nanostructures deposited at a) 1, b) 2 , c) 3 and d) 4 hours

Fig.3 shows the schematic diagram of the growth mechanism of ZnO nanostructures with regards to deposition time. The growth mechanism in CBD method comprises of ZnO nuclei and ZnO particles from solution and formed the ZnO nanostructures solid phase [22]. Theoretically, the chemical reactions involved in the formation of ZnO nanorods are summarized as below [23, 24]:

$$(CH_2)_6N_4 + 6\,H_2O \leftrightarrow 6CH_2O + 4NH_3 \quad (1)$$

$$NH_3 + H_2O \leftrightarrow NH_4^+ + OH^- \quad (2)$$

$$Zn(NO_3)_2 \rightarrow Zn^{2+} + 2NO_3^- \quad (3)$$

TABLE II
(100) PEAK POSITION, FWHM AND CRYSTALLITE SIZE AS CALCULATED FROM XRD

Deposition Time (Hour)	2 θ	FHWM (°)	D (nm)
1	32.32	0.3779	22.87
2	32.35	0.2786	31.03
3	32.10	0.2204	39.19
4	32.40	0.2204	39.22

$$Zn^2 + 4NH_3 \leftrightarrow Zn\,(NH_3)_4{}^{2+} \quad (4)$$

$$Zn^{2+} + 4OH^- \leftrightarrow Zn\,(OH)_4{}^{2-} \quad (5)$$

$$Zn\,(NH_3)_4{}^{2+} + 2OH^- \leftrightarrow ZnO + 4NH_3 + H_2O \quad (6)$$

$$Zn(OH)_4{}^{2-} \leftrightarrow ZnO + H_2O + 2OH^- \quad (7)$$

The HMT ($C_6H_{12}N_4$) is a non-ionic cyclic tertiary amine which hydrolyses in water at certain temperature and dissociate into formaldehyde (CH_2O) and ammonia (NH_3) as expressed in equation (1). The reaction of NH_3 in DI water caused the formations of hydroxide ions, OH^- (eq. (2)). while zinc nitrate hexahydrate $Zn(NO_3)_2.6H_2O$ will disintegrate into Zn^{2+} ions as derives in equation 3. The presence of NH_3 and OH^- anion from the reaction processes as stated in eq (1) and (2) caused Zn^{2+} cations from Zn $(N0_3)_2$. $6H_2O$ reacted. This Zn^{2+} ion required for ZnO nanostructures formation. The Zn^{2+} ion will react with OH^- and NH_4^+ ions and may lead to formation of aminezincate ion $[Zn\ (NH_3)_4]^{2+}$ and tetrahydroxozincate ions $Zn(OH_4)^{2-}$ as stated in equations (4) and (5) respectively. This $[Zn\ (NH_3)_4]^{2+}$ and $Zn(OH_4)^{2-}$ ions will act as ZnO nuclei. The dehydration process of $[Zn\ (NH_3)_4]^{2+}$ and $Zn(OH_4)^{2-}$ ions contributed to the formations of ZnO nanostructures as shown in equation (6) and (7) respectively.

The range of diameter and length of the ZnO nanostructures are shown in Table 1. It is evident that as the deposition hour increases, the diameter of ZnO nanostructures increased, with a small reduction seen from the nanostructures deposited at 4 hours. The same pattern can be seen for the length where it increases as the with the deposition time. The increasing diameter and length at 1 hour to 3 hour may be due to the consumption of (Zn^{+2}, OH^{-1}) with time. On the other hand, the slightly decreased of ZnO nanoflower length and diameter at 4 h need further detailed investigations to offer the growth mechanism.

B. XRD pattern

Fig. 4 shows the XRD patterns for ZnO nanostructures deposited at 1, 2, 3 and 4 hours respectively. It is ascertained that the peaks for ZnO occur at (100) and (101) at 2θ = 32.1~32.4° and 36.49° for all the samples. From the XRD results, the (100) peak is dominant for all samples. Besides that, it can be seen that the diffraction peaks are narrow and intense

corresponding to high crystalline nature of ZnO nanostructures. The (100) peaks can be associated to lateral growth of ZnO nanostructures [25].

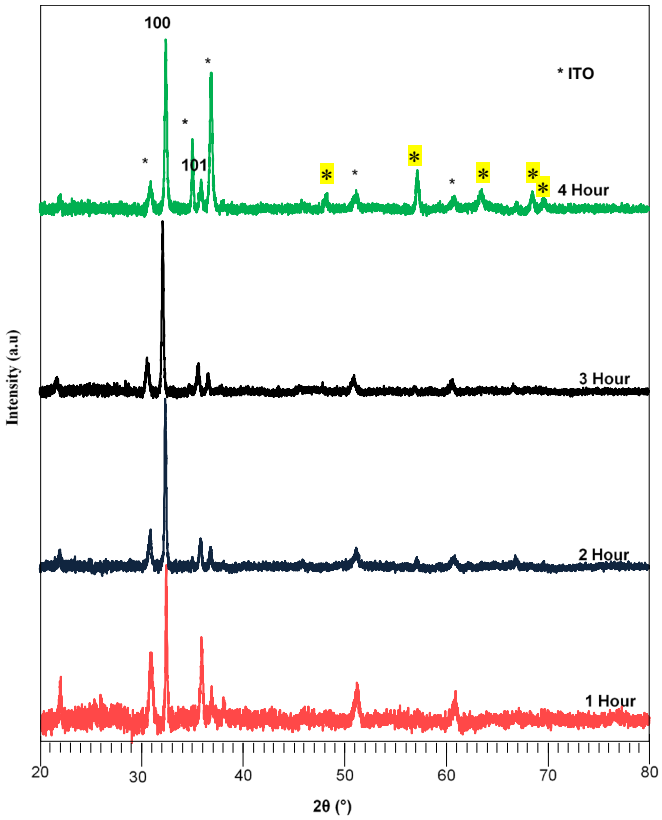

Fig. 4. XRD patterns for ZnO nanostructures deposited at a) 1hour, b) 2hours, c) 3hours and d) 4hours

The crystallite size *D* of the as deposited films was calculated for (100) using Equations (7) as below:

$$D = \frac{0.9\,\lambda}{\beta \cos\theta} \qquad (7)$$

where λ is the wavelength of the X-ray radiation source (0.15406 Å), β is FWHM and θ is the diffraction angle of (100) reflection, respectively. As can be seen in Table 2, the FWHM value of the samples decreased with the increasing deposition time to 3 h indicating the crystallinity improvement of the samples before became constant at 4 h. It is clear that the crystallite size of ZnO nanostructures increase with an increase in deposition time. Bidier et al discussed that this is due to restructure of interstitial defects (Zn and O) that reduce the vacancies (Zn and O) and lead to increase of ZnO nanostructures crystallite size [25]. The longer deposition time facilitates more interstitial defects restructuring that results in larger crystallite size.

C. EGFET pH Sensor Performance

Fig.5 (a), (b), (c) and (d) shows the transfer characteristic (I_D-V_{REF}) of ZnO nanostructures deposited at 1 to 4 hours immersed in buffer solution of pH 4, 7 and 10. This range of pH buffer is reported suffice for pH sensor measurement [26]. In this measurement, the drain voltage (V_D) was fixed at 500 mV while the reference voltage (V_{REF}) was swept from 1 to 2 V. From the figure, it can be seen that the transfer curve is not stable for the 1-hour sample since the I_D current for pH 10 is shifted to the left and nearly overlapping with that of pH 7. There are not much different on transfer curve results for 2, 3

TABLE III
THE VALUE OF SENSITIVITY AND LINEARITY FOR EACH THIN FILM AT DIFFERENT DEPOSITION TIME

Deposition Time (Hour)	Sensitivity (mV/pH)	Linearity
1	35.00	0.8523
2	35.00	0.9881
3	56.00	0.9997
4	43.00	0.9897

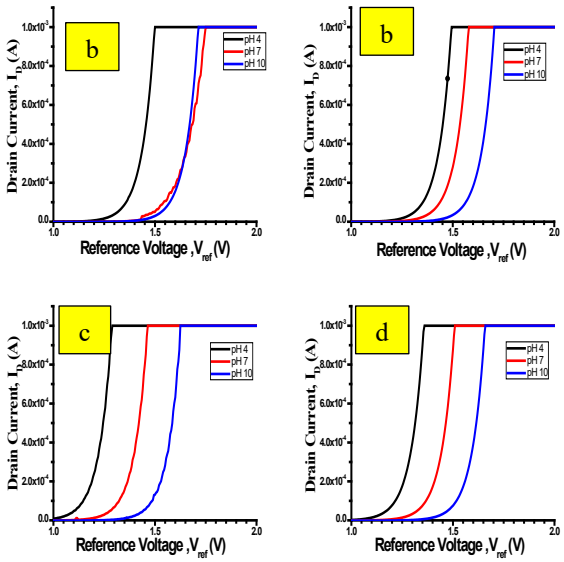

Fig. 5. Transfer characteristics (ID-VREF) of ZnO nanostructures deposited at a) 1hour, b) 2hours, c) 3hours and d) 4 hours for pH 4, 7 and 10.

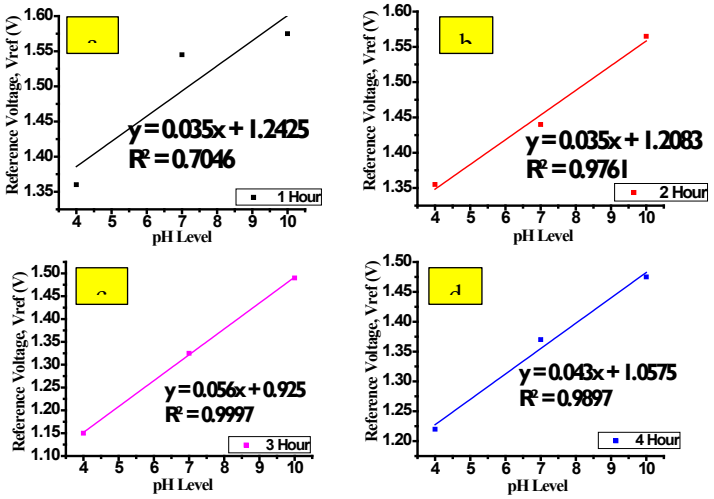

Fig. 6. Sensitivity and linearity for ZnO at a) 1hour, b) 2hours, c) 3hours and d) 4hours

and 4 h as shown in Fig.5 (a),(b) and (c) respectively. From transfer results, V_{REF} graph was plotted as shown in Figure 6. The value of V_{REF} was observed at ~100 µA of drain current (I_D) for each pH value 4, 7 and 10.

Fig.6 shows the gate voltage of the EGFET sensor during immersion in pH 4, 7, and 10 buffer solutions. The sensitivity and linearity of sensor were observed from slope and linear regression of V_{REF}-pH level graph respectively. Both values for each sensor are also tabulated in Table 3. The sensitivity and linearity increases with the deposition time with the highest sensitivity achieved is 56 mV/pH and the linearity is 0.9997. The increment may be attribute to the density of the ZnO nanostructures where it is evident from the FESEM results that the nanostructures density of the samples deposited for 1 and 2 hours were lower than 3 hours sample.

The high density provides high surface area that facilitates more contact between the membrane and the measurand thus more ion adsorptions occur that lead to higher sensitivity. The sensitivity parameter (β) is expressed in equation (8) below [1] :

$$\beta = \frac{2q^2 N_S \sqrt{\frac{K_a}{K_b}}}{KTC_{DL}} \quad (8)$$

where q is electron charge, N_S is surface site density, K_a and K_b are acidic and basic constants respectively. The Boltzmann constant, absolute temperature and capacitance of electrical double layer are represented by *K, T* and C_{DL} respectively. According to Eq. (8) ,besides the surface to volume ratio, the number of available site (N_s) on the surface of sensing membrane also contribute to better performance of pH sensitivity. In addition, the pH sensitivity also dependent on charge of surface potential (Ψ) between sensing membrane

and electrolyte interface as can be seen in equation (9) below:

$$\Psi = 2.303 \frac{KT}{q} \frac{\beta}{\beta+1} (pH_{PZC} - pH) \quad (9)$$

where the pH value at the point of zero charge is denotes by pH_{pzc}. Referring to the equation (8) and (9), it can be said that β directly proportional to N_s and Ψ. The relationship between *Ns* and Ψ is explained by site binding theory [1]. The site binding theory states that, the Ψ between sensing membrane and electrolyte surface can be altered by N_s on the sensing membrane. According to equation (9), the Ψ of the membrane increases with increasing of N_s. This Ψ improves the ion exchange process which lead to increase in accumulation of positive charge on surface membrane that enhance the pH sensitivity. Theoretically, the mechanism of pH sensor is dependent on surface reaction [1]. Thus the presence of both parameter (surface-to-volume ratio and *Ns*) are the crucial elements in increasing the pH sensor performance. This can also be related to the observation that the sensitivity of the sample immersed for 4 hour decreases to 43 mV/pH, and as can be seen from the FESEM result in Fig. 2(d), the decrease is probably due to lower density of ZnO nanostructures.

ZnO material is an inorganic metal oxide with amphoteric surface sites. These amphoteric surface sites are prone to the dissociation process between ZnO surface and electrolytes. The ZnO surface consists of OH hydroxyl group that perform a role as discrete sites for surface chemical reaction when in contact with the electrolyte solution.The surface charging mechanism begins when the hydroxyl group at ZnO surface adsorbed the hydroxyl ion to form positive or negative ion respectively. In aqueous medium and at alkaline pH, the chemisorbed protons (H^+) dissociate from the particle surface leaving a negatively charge surface with partially bonded oxygen atoms. At acidic medium, protons from the environment are likely to react with the particle surface resulting in a surface with positive charge. This formation in both alkaline and acidic mediums are described as follows [27, 28]

$$ZnO_{(S)} + 2H_2O = Zn(OH)_{3\,(S)}^{-} H^+(alkaline) \quad (10)$$

$$ZnO_{(S)} + H^+ = ZnOH_{(S)}^{+} (acid) \quad (11)$$

The sensing performance also have been tested using bare ITO as in order to confirmed that the high sensitivity obtained from this research are attributed by ZnO material. From the results, the pH sensitivity obtained using bare ITO is 22.0 mV/pH. Therefore this result proved that the high sensitivity obtained using ZnO nanostructures does not depend on ITO substrate.

The linearity of the 2-hour sample is 0.9881 which is higher compared to the 1-hour sample, 0.8523. This non-linearity also can be seen from the transfer curves result where the I_D current for the 1-hour sample in pH 7 and pH 10 are overlapping indicating that the output was unstable. This might be due to weak adhesion of ZnO nanostructures on glass substrate that cause the ZnO nanostructures to be peeled-off during the subsequent immersion in pH 4, 7 and 10 buffer solutions. The linearity of the 3-hour sample is the highest, 0.9997, approaching to 1, however, that of 4-hour sample decreases to 0.9897. Referring to the XRD results tabulated in Table 2, while the crystalline quality of the 3 and 4-hr samples is quite similar based on the FWHM, the sensor performance is different. Relating this to the FESEM images of the samples, this suggests that besides the crystalline quality, the sensing material density on the sensor surface also plays a crucial element to the overall sensor performance. The highest sensitivity achieved by 3 hours sample (56.0 mV/pH) is also higher than other ZnO sensing membrane reported in literature as tabulated in table 4.

V. CONCLUSION

ZnO nanoflowers were successfully deposited on ITO substrates using simple immersion CBD process at a low temperature of 95 °C, without any seed or catalyst layer. The deposited ZnO nanoflowers were then applied as the sensing membrane of an EGFET pH sensor. The growth of ZnO nanostructures was influenced by the immersion time. For 1 to 2-hours immersion time, ZnO nanostructures were formed scattered on the substrate surface. The pH sensing sensitivity for both samples were around 35 mV/pH but the linearity was found to be improved from 0.8523 to 0.9981 when the

TABLE IV
COMPARISON OF SENSITIVITY PERFORMANCE OF ZNO SENSING MEMBRANE USING VARIOUS METHODS

ZnO growth morphologies	Deposition Methods	Sensitivity (mV/pH)	Ref
ZnO Thin Film	Radio frequency Sputtering	0.8523	[28]
passivated i-ZnO nanorod array	Vapor cooling condensation	0.9881	[29]
ZnO Nanorods	Thermal Chemical Vapor Deposition	0.9997	[30]
ZnO Nanoflowers	Chemical Bath Deposition	0.9897	This work

immersion time was increased from 1 to 2 hours. The highest sensitivity and the best linearity were achieved from the sample deposited for 3 hours which produced highest density nanoflowers resulting in a high sensitivity of 56 mV/pH and linearity of 0.9997. The sensing performance can be related to the density of the ZnO structures on the substrate surface. High nanostructure density gives high surface area that facilitates more ion adsorption on the sensing membrane. The growth density of ZnO nanostructure was found highest for the 3-hour sample, which in turn produced the highest sensor performance.

ACKNOWLEDGMENT

This work was partially supported by the NRGS grant (Project Code: 600-RMI/NRGS 5/3 (7/2013)) of Ministry of Higher Education Malaysia. Authors would also like to thank the Institute of Research Management and Innovation (IRMI), UiTM for their support.

REFERENCES

[1] F. A. Sabah, N. M. Ahmed, Z. Hassan, and M. A. Almessiere, "Influence of CuS membrane annealing time on the sensitivity of EGFET pH sensor," *Materials Science in Semiconductor Processing,* vol. 71, no. Supplement C, pp. 217-225, 2017.

[2] F. A. Sabah, N. M. Ahmed, Z. Hassan, and M. A. Almessiere, "A novel CuS thin film deposition method by laser-assisted spray photolysis deposition and its application to EGFET," *Sensors and Actuators B: Chemical,* vol. 247, no. Supplement C, pp. 197-215, 2017.

[3] Q. Zhang *et al.*, "Polyaniline-functionalized ion-sensitive floating-gate FETs for the on-chip monitoring of peroxidase-catalyzed redox reactions," *Electrochimica Acta,* vol. 261, pp. 256-264, 2018.

[4] H. S. Rasheed, N. M. Ahmed, and M. Z. Matjafri, "Ag metal mid layer based on new sensing multilayers structure extended gate field effect transistor (EG-FET) for pH sensor," *Materials Science in Semiconductor Processing,* vol. 74, pp. 51-56, 2018.

[5] H. J. N. P. D. Mello and M. Mulato, "Effect of aniline monomer concentration on PANI electropolymerization process and its influence for applications in chemical sensors," *Synthetic Metals,* vol. 239, pp. 66-70, 2018.

[6] M.-S. Chae, J. H. Park, H. W. Son, K. S. Hwang, and T. G. Kim, "IGZO-based electrolyte-gated field-effect transistor for in situ biological sensing platform," *Sensors and Actuators B: Chemical,* vol. 262, pp. 876-883, 2018.

[7] S. Velanganni, S. Pravinraj, P. Immanuel, and R. Thiruneelakandan, "Nanostructure CdS/ZnO heterojunction configuration for photocatalytic degradation of Methylene blue," *Physica B: Condensed Matter,* vol. 534, pp. 56-62, 2018.

[8] N. Uria, N. Abramova, A. Bratov, F.-X. Muñoz-Pascual, and E. Baldrich, "Miniaturized metal oxide pH sensors for bacteria detection," *Talanta,* vol. 147, pp. 364-369, 2016.

[9] C. Schultealbert, T. Baur, A. Schütze, S. Böttcher, and T. Sauerwald, "A novel approach towards calibrated measurement of trace gases using metal oxide semiconductor sensors," *Sensors and Actuators B: Chemical,* vol. 239, pp. 390-396, 2017.

[10] D.-M. Kim, S. J. Cho, C.-H. Cho, K. B. Kim, M.-Y. Kim, and Y.-B. Shim, "Disposable all-solid-state pH and glucose sensors based on conductive polymer covered hierarchical AuZn oxide," *Biosensors and Bioelectronics,* vol. 79, pp. 165-172, 2016.

[11] V. L. Patil, S. A. Vanalakar, P. S. Patil, and J. H. Kim, "Fabrication of nanostructured ZnO thin films based NO2 gas sensor via SILAR technique," *Sensors and Actuators B: Chemical,* vol. 239, pp. 1185-1193, 2017.

[12] M. A. Zulkefle, R. A. Rahman, M. Rusop, W. F. H. Abdullah, and S. H. Herman, "Porous TiO2 Thin Film for Egfet pH Sensing Application," *2018,* EGFET; etching; pH sensor; porous; titanium dioxide vol. 7, no. 4.42, p. 3, 2018.

[13] B. Patella, R. Inguanta, S. Piazza, and C. Sunseri, "A nanostructured sensor of hydrogen peroxide," *Sensors and Actuators B: Chemical,* vol. 245, pp. 44-54, 2017.

[14] V. Galstyan, E. Comini, C. Baratto, G. Faglia, and G. Sberveglieri, "Nanostructured ZnO chemical gas sensors," *Ceramics International,* vol. 41, no. 10, pp. 14239-14244, 2015.

[15] S. A. Zaidi and J. H. Shin, "Recent developments in nanostructure based electrochemical glucose sensors," *Talanta,* vol. 149, pp. 30-42, 2016.

[16] A. El-Shaer, M. Abdelfatah, A. Basuni, and M. Mosaad, "Effect of KOH molarity and annealing temperature on ZnO nanostructure properties," *Chinese Journal of Physics,* vol. 56, no. 3, pp. 1001-1009, 2018.

[17] B. S. Mwankemwa, S. Akinkuade, K. Maabong, J. M. Nel, and M. Diale, "Effects of surface morphology on the optical and electrical properties of Schottky diodes of CBD deposited ZnO nanostructures," *Physica B: Condensed Matter,* 2017/07/18/ 2017.

[18] N. D. M. Sin, S. A. Kamaruddin, M. Z. Musa, and M. Rusop, "Effect of deposition time SnO2 thin film deposited using thermal CVD for humidity sensor application," in *2011 IEEE Symposium on Industrial Electronics and Applications*, 2011, pp. 459-462.

[19] N. E. A. Azhar, Z. Nurbaya, I. H. H. Affendi, M. N. Wahida, S. S. Shariffudin, and M. Rusop, "Effect of time deposition to the optical properties of ZnO nanotetrapods for OLED applications," in *2014 2nd International Conference on Electronic Design (ICED)*, 2014, pp. 157-160.

[20] P. K. Ghosh, S. F. Ahmed, B. Saha, and K. K. Chattopadhyay, "Effect of deposition time on optical properties of nanocrystalline CdS thin films synthesized via rf- sputtering technique," in *2007 International Workshop on Physics of Semiconductor Devices*, 2007, pp. 410-412.

[21] Z. Zheng, J. Lin, X. Song, and Z. Lin, "Optical properties of ZnO nanorod films prepared by CBD method," *Chemical Physics Letters,* vol. 712, pp. 155-159, 2018.

[22] P. R. Deshmukh, Y. Sohn, and W. G. Shin, "Chemical synthesis of ZnO nanorods: Investigations of electrochemical performance and photo-electrochemical water splitting applications," *Journal of Alloys and Compounds,* vol. 711, no. Supplement C, pp. 573-580, 2017.

[23] S. Syahirah, I. r. Ahmad Syakirin, M. Mohamad Hafiz, and Z. Ahmad Sabirin, "Influence of Growth Time and Temperature on the Morphology of ZnO Nanorods via Hydrothermal," *IOP Conference Series: Materials Science and Engineering,* vol. 99, no. 1, p. 012016, 2015.

[24] O. F. Farhat *et al.*, "A study of the effects of aligned vertically growth time on ZnO nanorods deposited for the first time on Teflon substrate," *Applied Surface Science,* vol. 426, no. Supplement C, pp. 906-912.

[25] "Effect of growth time on Ti-doped ZnO nanorods prepared by low-temperature chemical bath deposition," *Physica E: Low-dimensional Systems and Nanostructures,* vol. 88, p. 169, 2017.

[26] P. Salvo *et al.*, "Temperature and pH sensors based on graphenic materials," *Biosensors and Bioelectronics,* 2017.

[27] S. Al-Hilli *et al.*, "Zinc Oxide Nanorods as an Intracellular pH Sensor," in *ENS 2007*, Paris, France, 2007, pp. 38-43: EDA Publishing,https://hal.archives-ouvertes.fr/hal 00202509/documenthttps://hal.archives-ouvertes.fr/hal 00202509/file/ens07_038-2.pdf.

[28] A. Wei, L. Pan, and W. Huang, "Recent progress in the ZnO nanostructure-based sensors," *Materials Science and Engineering: B,* vol. 176, no. 18, pp. 1409-1421, 2011.

Aimi Bazilah Binti Rosli received her BSc. Degree and Msc in Electrical Engineering from Universiti Teknologi MARA (UiTM), Malaysia. Previously, she worked as Research assistant at UiTM from 2013-2014 and Part-time lecturer in Faculty Electrical Engineering, Universiti Teknologi MARA. She currently a PhD in Electrical Engineering at same university. Her study were focused on fabrication and characterization of sensing material.

Ahmad Syakirin bin Ismail@Rosdi received his BSc. Degree and Msc in Electrical and Electronics Engineering from Universiti Teknologi MARA (UiTM), Malaysia in 2010-2015. Currently, he is a doctoral student under the supervision of Dr. Mohamad Hafiz Mamat also at Universiti Teknologi MARA (UiTM). His research interest is on the fabrication of composite material-based sensors.

Zaiki Awang (M'97 – SM'03) received the BSc and MSc degrees in microwave engineering from the University of Portsmouth, England in 1984 and 1987 respectively, and the PhD degree from the University of Leeds in 1995. His doctoral work involved implementation of sol-gel materials in the design of bulk acoustic wave resonators for microwave integrated circuits. Since August 1985 he has been with Universiti Teknologi MARA, where he is currently Professor of Microwaves with the Faculty of Electrical Engineering. He was the Deputy Dean from 1996 to 2002, and Head of Communication Engineering Department from 1998 to 2002. He is presently Director of Microwave Research Institute of the university. He was a Visiting Scholar at Illinois Institute of Technology from August to November 2009. He is the author of two books - *Microwave Engineering for Wireless Communications* (Pearson/Prentice Hall, 2006), and *Microwave Sub-System Design* (Springer, 2014). He has also written several book chapters, and more than 180 technical papers. His research interests include microwave electronics, advance microwave materials, microwave ultrasonics and computational electromagnetics.

Prof. Awang is an active member of the IEEE. He was the 2008-2010 Chair of IEEE Malaysia Section, and is a founding member and past Chair of IEEE Antennas and Propagation/Microwave Theory and Techniques/Electromagnetic Compatibility Malaysia Chapter. He is Head of Commission of Electronics and Photonics, and Malaysian representative for the Fields and Waves Commission of International Union of Radio Science (URSI). He is the founding member of IEEE International RF and Microwave (RFM) and Asia Pacific Applied Electromagnetics (APACE) series of conferences in Malaysia.

Muhammad Farid Abdul Khalid received the B.Eng. (Hons) degree in microelectronics engineering from the Universiti Kebangsaan Malaysia (UKM), Bangi, Malaysia in 2002, the M.Sc. (Eng.) degree in microelectronic systems and telecommunications from the University of Liverpool (UoL), Liverpool, United Kingdom in 2004, and the Ph.D. degree in communication and electronics engineering from the Royal Melbourne Institute of Technology (RMIT), Melbourne, Australia in 2014.

In 2005, he joined the Faculty of Electrical Engineering, Universiti Teknologi MARA, Shah Alam, Malaysia as a Lecturer and was promoted to Senior Lecturer in 2010. In 2014, he joined the Microwave Research Institute (MRI), Universiti Teknologi MARA, Shah Alam, Malaysia as a Member and currently serves as a Research Coordinator. His research interests include microwave passive devices, microwave modeling, and synthesis, characterization, and fabrication of high frequency thin film materials.

Shafinaz Sobihana Shariffudin received her BEng (hons) degree in Microelectronics Engineering and MSc in Microelectronics from Universiti Kebangsaan Malaysia in 2002 and 2003, respectively. She received her PhD in Electrical Engineering specializing in Nanoelectronics from Universiti Teknologi MARA in 2016. Previously, she worked as a lecturer at Universiti Teknikal Malaysia (formerly known as KUTKM) from 2003 to 2004. After that she moved to Universiti Industri Selangor and served as a lecturer from 2004 to 2005. Shafinaz is currently a senior lecturer in Faculty of Electrical Engineering, Universiti Teknologi MARA since 2005. She is now engaged with Nanoelectronic Center (NET) in the faculty and has contributed to many research publications in the area of nanoelectronics and materials fabrication. Her research interest includes thin films of organic and inorganic materials, nanostructured materials, organic light emitting diodes and organic solar cells.

Sukreen Hana Herman received her B.Eng degree in Electrical, Electronics and Information engineering and M.Eng in Electronics and Computer Science from Kanazawa University, Japan in 1999 and 2004, respectively. She received her PhD in Materials Science in 2009 from the Japan Andvanced Institute of Science and Technology (JAIST). Sukreen received the Malaysian Public Service Department (JPA) Scholarship for her degree, Panasonic Scholarship for her Master and the Japan Monbukagakusho (MEXT) Scholarship for her PhD. Sukreen was with Sharp-Roxy before pursuing her Master. She joined Universiti Teknologi MARA (UiTM) in 2004 and now is the senior lecturer at the Center for Electronic Engineering Studies, Faculty of Electrical Engineering, UiTM. She heads the Integrated Sensor Research group in the Faculty. Her research interests include fabrication and characterization of semiconductor materials, sensing membranes and nanostructured materials. Although her work explores various methods of fabrication and growth, her early work focused on sputtering deposition where she designed and developed an RF sputtering machine for her Master research. Sukreen is one of the authors for more than 170 articles and conference proceedings and has received various major awards in invention and innovation exhibition and competitions.